ELECTRO-THERMO-MECHANICAL ANALYSIS OF CB/PLA SAMPLES MADE BY ADDITIVE MANUFACTURING

Laurane Roumy[1,2,3]*, Fabienne Touchard[1], Damien Marchand[1], Thuy Quynh Truong Hoang[2] and Francisca Martinez-Hergueta[3]

[1] Institut PPRIME, CNRS-ENSMA-Université de Poitiers, Dpt Physique et Mécanique des Matériaux, ENSMA, 1Av. C. Ader, B.P. 40109, 86961 Futuroscope Cedex, France,
fabienne.touchard@ensma.fr, damien.marchand@ensma.fr
[2] ESTACA, Pôle Mécanique des Structures Composites et Environnement, Ecole d'ingénieurs, France,
thuy-quynh.truong-hoang@estaca.fr
[3] School of Engineering, Institute for Infrastructure and Environment, University of Edinburgh, UK,
francisca.mhergueta@ed.ac.uk
* Corresponding author (laurane.roumy@ensma.fr)

Keywords: 3D-printing, Joule effect, Optimisation, Tensile behaviour

ABSTRACT

Additive manufacturing of smart materials reacting to an external stimulus is known as 4D-printing, the fourth dimension referring to time. Thus, Fused Deposition Modelling (FDM) of thermally activated Shape Memory Polymers (SMP) is used to create structures that can change their shape to a preprogrammed one when their temperature rises above their glass transition temperature. In particular, these changes in temperature can be self-induced by Joule effect in multifunctional materials such as carbon black nanoparticles reinforced polymers. Applications in numerous fields are possible: aerospace, medicine, drones or robotics. The reliability of electro-induced heating of shape memory polymers is an issue to be considered in the development of 3D printed actuators. In this study, electrical, thermal and mechanical characteristics of a CB/PLA nanocomposite are investigated. The thermal properties of the material are characterised thanks to different means. The influence of Joule effect on the heating of the material is studied through the application of different values of voltage on rectangular shape samples. Finally, the mechanical behaviour of the samples is studied through cyclic tensile tests. Results show that the higher the voltage, the higher the temperature within the specimens and the faster the heating and cooling rates. Tensile cyclic tests show a degradation of secant modulus and permanent strains after stress releasing. An analytical modelling is also developed to predict the thermal behaviour of the material. This study paves the way for the design of a 4D printed device remotely controlled by electricity.

1 INTRODUCTION

Additive manufacturing, also known as 3D-printing, is a process that consists in creating three-dimensional structures by applying the material layer by layer. Less waste production, cheaper costs, easier manufacturing of complex structures and customizable prototypes are its main benefits compared to conventional manufacturing methods [1]. Several techniques exist depending on the application and different kinds of materials can be used such as metals, ceramics, concrete or polymers and polymer-based composites [2]. For these latter, the Fused Filament Fabrication (FFF) (or Fused Deposition Modelling (FDM)) method is the most widespread process because of its affordability and ease of use [3]. It consists in heating the thermoplastic polymer above its melting temperature and depositing it as filaments through a nozzle on a heated bed to create a layered structure. Among the polymers, the Shape Memory Polymers (SMP) are a category of materials that have the ability of changing their shape over time under the influence of an external stimulus [4]. The stimulus can be for instance humidity, light or heat. Materials can be heated by an external source, or thanks to magnetic, or conductive fillers [5]. The combination of SMP and 3D-printing is often called 4D-printing, the fourth dimension referring to time [6]. 4D-printing is a dynamic field of research where an abundance of applications have been imagined including soft robotics, medicine, self-healing structures or space applications [7].

In this study, the focus is put on electro-activated SMPs. These materials have the benefits of long-range control and internal heating achieved through the integration of conductive particles such as silver particles, carbon nanotubes (CNT) or carbon black (CB) into a thermoresponsive polymer [8]. In particular, CNT/PLA and CB/PLA [9] composites are used in several studies for 4D-printing. Indeed, the polylactic acid (PLA) is a polymer commonly manufactured by FFF and has the specificity of being a thermoactivated SMP. Electro activation works thanks to Joule heating created by the conductive particles within the material. Therefore, questions on electrical, physical, thermal and mechanical properties of such material are essential. A detailed study of the influence of Joule heating on CB/PLA 3D printed samples by applying three different voltages during electrical cyclic tests completed by an analytical modelling and the study of the consequences at the micro-scale has been published recently [10].

In the present paper, a physical and thermal characterisation of a commercially available filament was firstly conducted, followed by an optimisation of the measurement of the electrical resistance of the samples and the study of the influence of the raster angle on 1mm-thick rectangular samples. An analysis of the Joule effect was then carried out by applying different voltage values and a predictive analytical modelling was developed. The mechanical properties of 3D printed specimens were also studied.

2 MATERIAL AND METHODS

2.1 Carbon black/PLA and 3D printed samples

A carbon black/polylactic acid (CB/PLA) filament from ProtoPasta was used with Ultimaker printers and a nozzle diameter of 0.8mm. Spools with filaments with a diameter of 2.85mm were used and CAD files were created thanks to CATIA V5 and sliced with the Ultimaker Cura software. Rectangular shape samples with a dimension of $70x20x1mm^3$ were manufactured with a 0° raster angle which means that the printed filaments were deposited along the longitudinal dimension, or a 90° raster angle which is perpendicular to the previous printing direction. The infill density was set at 100%, the nozzle temperature at 210°C and the bed temperature at 60°C.

2.2 Physical characterisation

Thermal characterisation was performed by means of a Differential Scanning Calorimetry (DSC) Q20 from TA Instruments. The samples were heated between 10°C and 200°C at a heating rate of 10°C/min.

The determination of the ratio of carbon black fillers can be determined by Thermogravimetric Analysis (TGA) [11]. The experiment was conducted with a Setsys Evolution machine on a 193.15mg sample of raw CB/PLA filament. The carbon black particles concentration was determined after the material was heated at 10°C/min within a temperature range of [25-600°C] under a nitrogen atmosphere with a flow rate of 50mL/min.

2.3 Electrical setup and thermal measurements

To ensure an optimum contact between the material and the electrical circuit, the samples were secured thanks to washers and nuts in galvanized steel fixed with a couple of 2N.m applied by a FACOM torque wrench. Thirty seconds after the contact was made, the electrical resistance was measured by a Keithley 2700 multimeter with a four-point probe method.

For the analysis of the Joule effect, the specimens were heated thanks to a DC power supply AL936N applying different voltage values. The voltage was applied during three minutes and thirty seconds and then switched off for the same period. Temperature was measured both by a K-type thermocouple with a diameter of 0.25mm and an infra-red Infratech Variocam HD Head 680 camera. The evolution of the electrical resistance was measured by a Keithley 2700 multimeter with a 4-point probe method during the cooling phase or the measurement of the current following Eq.1 during the heating phase:

$$U = R.I \tag{1}$$

where U is the applied voltage, I is the current and R is the electrical resistance.

2.4 Tensile tests

For the mechanical analysis, cyclic tensile tests were conducted on an INSTRON 3369 with a crosshead speed of 1mm/min. Longitudinal and transversal strains were measured with INSTRON extensometers with a gauge length of 50mm and 20mm respectively. 3D-printed samples with a dimension of 175x20x3mm^3 and three raster angles 0°, 90° or ±45° were tested.

3 RESULTS AND DISCUSSION

3.1 Characterisation of the as-received material

A physical and thermal characterisation of the raw CB/PLA filament was conducted. The TGA thermogram is shown in Fig. 1. The thermal degradation temperature T_d of the polymer matrix is comprised between 332°C and 490°C (Table 1). Three different stages can be described. A drastic mass loss is detected around 330°C due to the degradation of PLA. Then, another progressive change is observed around 400°C, corresponding to the degradation of a polymer blend added during the manufacturing of the filament and specified in the supplier's safety data sheet. The third stage is above 500°C where only the carbon black remains. Thus, the carbon ratio in weight τ_{CB} was measured equal to 21.5±0.1% (Table 1), which corresponds to the proportion detailed in the safety data sheet.

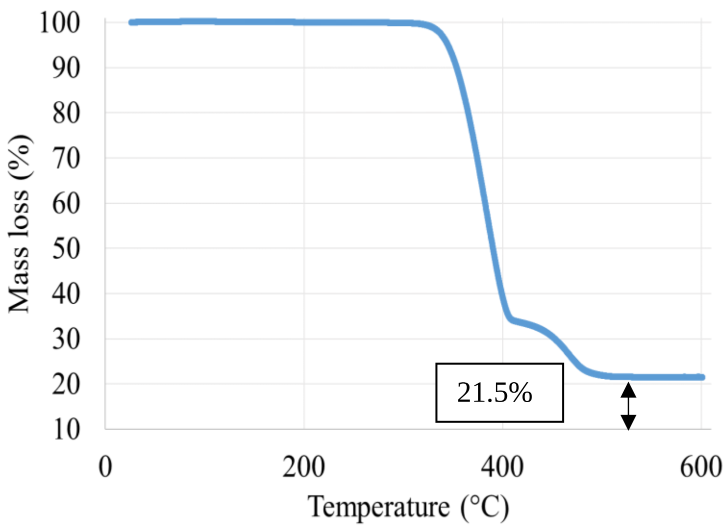

Figure 1: TGA thermogram of the as-received CB/PLA filament.

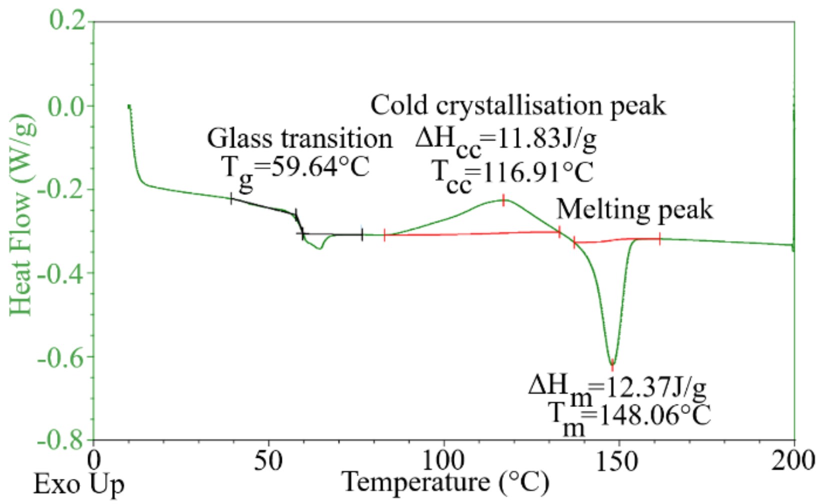

Figure 2: DSC thermogram of the as-received CB/PLA filament.

Thermal degradation temperature (°C)	Carbon black ratio in weight τ_{CB} (%)	Glass transition temperature T_g (°C)	Melting temperature T_m (°C)	Cold crystallisation temperature T_{cc} (°C)	Crystallinity ratio χ_v (%)
[332;490]	21.5±0.1	59.64±0.5	148.06±0.5	116.91±0.5	0.7±0.7

Table 1: Characteristics of the as-received CB/PLA material

The DSC measurements (Fig.2) allowed the determination of the glass transition temperature T_g, the melting temperature T_m and the cold crystallisation temperature T_{cc}, all reported in Table 1. The crystallinity ratio χ_v was calculated thanks to the following equation (Eq.2)[12]:

$$\chi_v = \frac{\Delta H_m - \Delta H_{cc}}{\Delta H_m^0 \times (1 - \tau_{CB})} \times 100\% \tag{2}$$

The enthalpy of melting ΔH_m and the enthalpy of crystallisation ΔH_{cc} were obtained by measuring the surface areas on the DSC thermogram and the carbon ratio in weight τ_{CB} was measured previously. ΔH_m^0 corresponds to the enthalpy of melting of a fictive 100% crystallised PLA, equal to 93.6J/g according to the work of Solarski et al.[13]. A crystallinity ratio χ_v of about 0.7% was measured for the raw CB/PLA filament (Table 1), which means that the material is amorphous.

3.2 Reproducibility and optimisation of the electrical resistance

Thanks to the procedure described in Section 2.3 to optimise the contact between the 3D printed samples and the electrical setup, results showed that the standard deviation of the measured electrical resistance for a given sample did not exceed 7Ω, demonstrating that the method was reproducible. In addition, standard deviation between the mean resistance values of the three different samples was only 4Ω, showing that there was no high dispersion from one sample to another. Thus, the resistance of the samples was reproducible and equal to 182Ω, showing that FDM is reliable to elaborate conductive samples.

The influence of the raster angle was also studied. A sample was printed with a raster angle of 90°. It appeared that the resistance of this specimen was increased by 75% in comparison with the 0° sample (319±3Ω versus 182±4Ω). It can be explained by the fact that the electricity is better conducted along a printed filament than between adjacent ones. Thus, the 0° raster angle was used in the following.

3.3 Analysis of the electro-thermal behaviour

3.3.1 Selection of the voltage value

In order to choose the voltage values that will be used for testing the Joule effect, voltages from 10V to 35V were applied on a CB/PLA sample. After about 3min, the maximum temperature values were reached and measured in the middle of the specimen by an infrared camera. The tests showed that the glass transition temperature could be reached by applying only 20V and the temperature could reach up to 110°C when applying 30V. The objective of this study was to analyse the behaviour of CB/PLA in order to use its shape memory effect. Therefore, the samples need to be heated above the material glass transition temperature, which was determined close to 60°C, while remaining below the melting temperature equal to 148°C (Table 1). As expected, the higher the voltage, the higher the temperature reached within the sample. Thus, the voltage of 30V was selected for the Joule heating study in the following experiments.

3.3.2 Joule heating

CB/PLA samples were printed with a 0° raster angle and subjected to a voltage value of 30V. The reproducibility of the experiment was successfully verified and the evolution of the temperature measured at the central point of one of the samples and an IR camera image are shown in Fig.3. This curve allowed the determination of the heating (HR) and cooling rates (CR) (Fig. 3). Results showed that the samples are heated at a rate of 2.6±0.1°C/s and cooled down at a rate of 1.5±0.1°C/s for an applied voltage of 30V. While the heating is due to the Joule effect, the cooling of the samples is explained by convection exchanges with the environment.

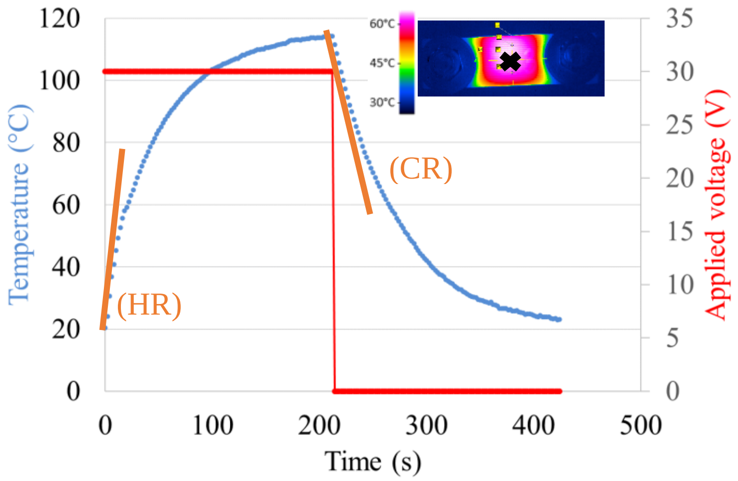

Figure 3: Evolution of the temperature in the centre of a 0° sample under a 30V voltage applied during 3min30s and then stopped. HR: heating rate; CR: cooling rate.

Thermal images captured by the infrared camera allowed the analysis of the temperature field due to the Joule effect (Fig. 3). The circular shapes on both sides of each cartography correspond to the presence of the nuts. It can be seen in Fig. 3, along the longitudinal line, a drop of the temperature value at the edges of the sample. This is due to the presence of the nuts, which secured the sample to the electrical setup. Looking closely at the image in Fig. 3, the temperature is slightly higher at the top of the sample compared to the bottom. This is due to the fact that the sample is placed vertically. The observed phenomenon is therefore explained by the natural convection of the air, which pushes the warmest lighter air upwards. However, results show that, in the two directions, the overall distribution of temperature tends toward a plateau in the central part of the sample, demonstrating that the temperature due to the Joule effect is quite homogeneous in the gauge length of the sample.

3.3.3 Predictive analytical modelling

In order to predict the Joule heating and the cooling regime of our samples, an analytical modelling based on the conservation law of energy [10] was developed (Eq.3):

$$dQ_G = dQ_S + dQ_E \tag{3}$$

where dQ_G is the generated energy, dQ_S is the stored energy and dQ_E is the energy exchanged with the environment. The predominant heat transfers were assumed to be due to convection (Eq. 4) and conduction (Eq. 5):

$$\varphi_1 = hSd\theta \tag{4}$$

$$\varphi_2 = \frac{\lambda A}{l_c} d\theta \tag{5}$$

with h the convection coefficient of air, S the surface of exchange with the environment, λ the thermal conductivity of the material, A the surface of exchange and l_c the length considered for the conduction. Moreover, the electrical resistance depends on the temperature [10]. Thus, the differential equation to solve for the heating regime is (Eq.6):

$$\frac{V_0^2}{mC_pR_0} = [1 + b(\theta(t) - \theta_0)] \times \left[\frac{d\theta}{dt} + \left(\frac{1}{\tau} + \frac{\lambda A}{l_c m C_p}\right)(\theta(t) - \theta_{amb})\right] \tag{6}$$

with τ the characteristic time given by Eq.7:

$$\tau = \frac{mC_p}{Sh} \tag{7}$$

During the cooling regime, the power supply is switched off, meaning that the generated energy is null. The Eq.6 becomes then (Eq.8):

$$\theta_{amb}\left(\frac{1}{\tau} + \frac{\lambda A}{emC_p}\right) = \frac{d\theta}{dt} + \theta(t)\left(\frac{1}{\tau} + \frac{\lambda A}{emC_p}\right) \tag{8}$$

Using the experimental parameters (Table 1), it was possible to solve the Eq. 6 thanks to the solver ode45 from MATLAB and calculate the cooling regime deducing the first order differential equation from Eq. 8. The obtained curves are plotted in Fig.4 and compared with experimental data measured in the middle of a sample subjected to 30V. Results show that the analytical model closely predicts the experimental measurements for the applied voltage. A slight difference is observed during the heating, due to a small disturbance around the glass transition temperature explained by the shape memory behaviour of the material. In addition, the sample is predicted to cool more slowly according to the analytical model. It is probably due to the fact that the curvature of the washers was not considered into the calculation of the exchange surfaces for convection and conduction, thus underestimating their influence on the cooling process. However, the overall tendency is reproduced and it demonstrates that this analytical model, taking into account the variation of electrical resistance with the temperature [10], can be used as a first approach to predict the behaviour of a CB/PLA sample subjected to electrical power.

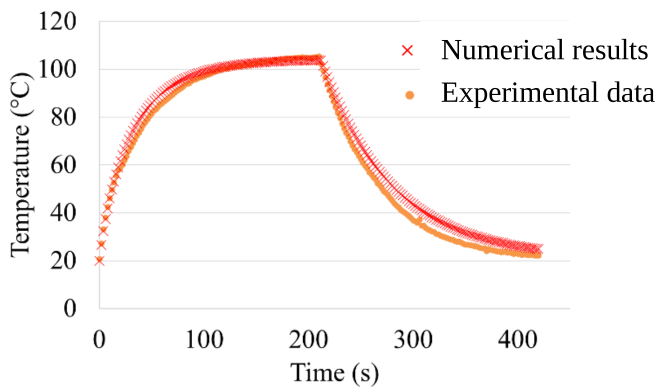

Figure 4: Analytical model and experimental data of the evolution of temperature for a CB/PLA sample subjected to a voltage of 30V during 3min30s.

3.4 Cyclic tensile tests

Quasi-static and cyclic tensile tests were performed on samples printed with 0°, 90° or ±45° raster angles. Figure 5 shows an example of a stress-strain curve obtained for the 0° raster angle.

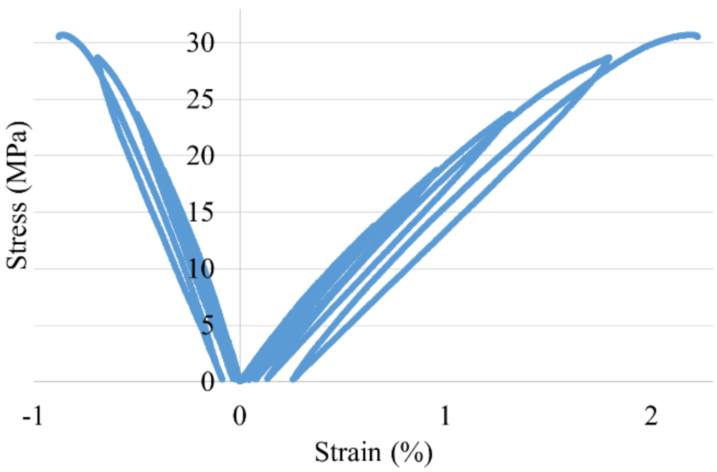

Figure 5: Cyclic tensile curve of 0° raster angle CB/PLA specimen.

For each cycle, the secant modulus is determined by using the extreme values. The first cycle is performed in the elastic field while the seventh cycle is conducted up to failure. During tensile cyclic tests, the secant modulus of the first cycle is about 2568±81MPa. This value falls to 1883±62MPa for the final cycle. Furthermore, the residual strain increases with the number of cycles. Mechanical properties of CB/PLA are therefore found to degrade under cyclic tensile tests, demonstrating the development of a plastic strain as well as damage within the specimen.

The failure stress obtained for the 0° raster angle was 26.84±2.01MPa and the elongation at break 3.47±0.39%. Work is in progress for analysing more precisely the secant modulus evolution and the damage development during tensile loading for the three raster angles.

4 CONCLUSIONS

An analysis of the Joule effect on 3D printed CB/PLA samples was presented in this work as well as a preliminary study of their mechanical behaviour. First, an in-depth characterisation of the as-received material was conducted. 3D printed CB/PLA samples were then manufactured and a specific electrical set-up with thermal camera was developed in order to ensure the reproducibility of the measurements. Results showed the importance of the raster angle to optimise the electrical conductivity. Knowing the glass transition temperature, it allowed the determination of relevant voltages to heat the 3D printed CB/PLA at a temperature to which it would be able to perform the shape memory effect: above 20V. Thus, a voltage of 30V was chosen for the study. The analysis of the full-field thermal maps showed a quasi-homogeneous distribution within the gauge length of the sample. The heating and cooling behaviour of the samples was also proven to be predictable thanks to an analytical modelling based on the conservation law of energy. Quasi-static and cyclic tensile tests were performed on 3D printed CB/PLA samples with 0°, 90° and ±45° raster angles and the evolution of the secant modulus and residual strain were also observed. Finally, this study shows that CB/PLA is a good candidate for 4D printing: it has a low glass transition temperature that enables its heating by Joule effect with reasonable voltages. Knowing the mechanical properties would help developing relevant applications. The obtained results pave the way for designing reliable and durable 4D printed CB/PLA actuators.

ACKNOWLEDGEMENTS

This work was supported by the Defense Innovation Agency (AID) of the French Ministry of the Armed Forces through the grant [AID-2021 65 0045].

REFERENCES

[1] T. D. Ngo, A. Kashani, G. Imbalzano, K. T. Q. Nguyen, and D. Hui, ‘Additive manufacturing (3D printing): A review of materials, methods, applications and challenges’, *Composites Part B: Engineering*, vol. 143, pp. 172–196, Jun. 2018, doi: 10.1016/j.compositesb.2018.02.012.

[2] X. Wang, M. Jiang, Z. Zhou, J. Gou, and D. Hui, ‘3D printing of polymer matrix composites: A review and prospective’, *Composites Part B: Engineering*, vol. 110, pp. 442–458, Feb. 2017, doi: 10.1016/j.compositesb.2016.11.034.

[3] S. Valvez, P. N. B. Reis, L. Susmel, and F. Berto, ‘Fused Filament Fabrication-4D-Printed Shape Memory Polymers: A Review’, *Polymers*, vol. 13, no. 5, Art. no. 5, Jan. 2021, doi: 10.3390/polym13050701.

[4] G. Ehrmann and A. Ehrmann, ‘3D printing of shape memory polymers’, *J Appl Polym Sci*, vol. 138, no. 34, p. 50847, Sep. 2021, doi: 10.1002/app.50847.

[5] Y. Liu *et al.*, ‘Remotely and Sequentially Controlled Actuation of Electroactivated Carbon Nanotube/Shape Memory Polymer Composites’, *Adv. Mater. Technol.*, vol. 4, no. 12, p. 1900600, Dec. 2019, doi: 10.1002/admt.201900600.

[6] I. T. Garces and C. Ayranci, ‘Active control of 4D prints: Towards 4D printed reliable actuators and sensors’, *Sensors and Actuators A: Physical*, vol. 301, p. 111717, Jan. 2020, doi: 10.1016/j.sna.2019.111717.

[7] A. Mitchell, U. Lafont, M. Hołyńska, and C. Semprimoschnig, ‘Additive manufacturing — A review of 4D printing and future applications’, *Additive Manufacturing*, vol. 24, pp. 606–626, Dec. 2018, doi: 10.1016/j.addma.2018.10.038.

[8] A. Kausar and R. Taherian, ‘Electrical Conductivity Behavior of Polymer Nanocomposite with Carbon Nanofillers’, in *Electrical Conductivity in Polymer-Based Composites: Experiments, Modelling and Applications*, Elsevier, 2019, pp. 41–72. doi: 10.1016/B978-0-12-812541-0.00003-3.

[9] C. A. Garcia Rosales *et al.*, ‘3D printing of shape memory polymer (SMP)/carbon black (CB) nanocomposites with electro-responsive toughness enhancement’, *Mater. Res. Express*, vol. 5, no. 6, p. 065704, Jun. 2018, doi: 10.1088/2053-1591/aacd53.

[10] L. Roumy, F. Touchard, D. Marchand, T. Q. Truong Hoang, and F. Martinez-Hergueta, ‘Durability of Joule effect of 3D printed carbon black/polylactic acid: Electrical cyclic tests and

analytical modelling', *International Journal of Fatigue*, vol. 173, p. 107677, Aug. 2023, doi: 10.1016/j.ijfatigue.2023.107677.

[11] J. Luo, H. Wang, D. Zuo, A. Ji, and Y. Liu, 'Research on the Application of MWCNTs/PLA Composite Material in the Manufacturing of Conductive Composite Products in 3D Printing', *Micromachines*, vol. 9, no. 12, p. 635, Nov. 2018, doi: 10.3390/mi9120635.

[12] L. Wang, J. Qiu, E. Sakai, and X. Wei, 'The relationship between microstructure and mechanical properties of carbon nanotubes/polylactic acid nanocomposites prepared by twin-screw extrusion', *Composites Part A: Applied Science and Manufacturing*, vol. 89, pp. 18–25, Oct. 2016, doi: 10.1016/j.compositesa.2015.12.016.

[13] S. Solarski, M. Ferreira, and E. Devaux, 'Characterization of the thermal properties of PLA fibers by modulated differential scanning calorimetry', *Polymer*, vol. 46, no. 25, pp. 11187–11192, Nov. 2005, doi: 10.1016/j.polymer.2005.10.027.